Optics Communications 282 (2009) 2339–2342

Contents lists available at ScienceDirect

Optics Communications

journal homepage: www.elsevier.com/locate/optcom

Stable all-fiber photonic temporal differentiator using a long-period fibergrating interferometer

Radan Slavík [a,b,*], Yongwoo Park [c], David Krčmařík [a], José Azaña [c]

[a] Institute of Photonics and Electronics, Academy of Sciences of the Czech Republic, v.v.i., Chaberská 57, 182 51 Prague, Czech Republic
[b] CESNET a.l.e., Zikova 4, 160 00 Prague 6, Czech Republic
[c] Institut National de la Recherche Scientifique (INRS), Centre Energie, Matériaux et Télécommunications, Montréal, Québec, Canada H5A 1K6

ARTICLE INFO

Article history:
Received 16 January 2009
Received in revised form 26 February 2009
Accepted 26 February 2009

Keywords:
Optical pulse shaping
Optical fiber filters
Passive filters
Gratings

ABSTRACT

A novel configuration of all-fiber photonic temporal differentiator optimized for tens-of-gigahertz processing bandwidth is suggested and experimentally demonstrated. This device covers the gap in terms of processing bandwidth between the two previously-demonstrated all-fiber designs, namely the fiber Bragg grating-based differentiator (<20 GHz) and that based on a uniform long-period fiber grating (>100–200 GHz).

1. Introduction

Temporal differentiation of optical signals has been recently reported as a basic building block for a variety of ultrafast all-optical signal processing operations [1–7] of interest in a wide range of fields, including fiber-optics telecommunications. Applications directly relevant to telecommunications include, e.g., novel methods for complete optical signal characterization in ultrahigh-bit-rate fiber-optics telecommunication links [8], flat-top pulse re-shaping for all-optical switching and wavelength-conversion operations [9], and Hermite–Gaussian pulse generation [4], which comprises Gaussian monocycle generation for ultra-wideband (UWB) microwave communications [10].

Basically, two main groups of methods have been previously implemented for photonic temporal differentiation. Methods included in the first group are based on various schemes incorporating nonlinear interaction in semiconductor optical amplifiers (SOA) [3,6]. These methods provide the differentiation of the optical intensity profile of the input waveform. The second approach, of our interest here, provides the differentiation of the optical signal's complex field envelope (including its amplitude and phase) and is based on the use of a customized linear optical filter. In particular, to get the required functionality, we need a linear optical filtering device providing a spectral transfer function of the form

$$H_t(\omega-\omega_0)\approx -i(\omega-\omega_0), \tag{1}$$

where ω is the optical frequency variable, ω_0 is the carrier optical frequency of the signal to be processed, and $i=\sqrt{-1}$ [1,4]. Its Fourier counterpart represents the first-order temporal derivative of the complex envelope of the input optical signal. By analyzing Eq. (1), we see that the required linear optical filter has a transfer function that depends linearly on the frequency variable ω and reaches zero at the signal's carrier frequency ω_0. It is worth noting that this implies an exact π-phase jump in the filter transmission at the central frequency ω_0 [1]. Notice also that as evidenced by the frequency transfer function in Eq. (1), an optical differentiator is a notch optical filter (i.e. a 'band-stop' filter).

These differentiators were demonstrated using fiber Bragg gratings with a π-phase shift, π-FBGs, operating in reflection [5], uniform long-period fiber gratings, LPFGs [4], and Michelson interferometers based on bulk-optics setups [7]. The required filtering characteristics are obtained around the filter 'zero-transmission' frequency (resonant frequency in a LPFG set to full coupling condition, resonant frequency in a π-FBG, or destructive-interference frequency in a Michelson interferometer), which has to be set precisely to ω_0. Differentiators based on a π-FBG exploit the notch filtering characteristic induced by the phase shift in the grating reflection bandwidth and as a result, they were found to provide relatively limited bandwidth (typically <20 GHz) [5]; in

* Corresponding author. Address: Institute of Photonics and Electronics, Academy of Sciences of the Czech Republic, v.v.i., Chaberská 57, 182 51 Prague, Czech Republic. Tel.: +420 266 773 503; fax: +420 284 680 222.
E-mail address: slavik@ufe.cz (R. Slavík).

0030-4018/$ - see front matter © 2009 Elsevier B.V. All rights reserved.
doi:10.1016/j.optcom.2009.02.069

contrast differentiators based on uniform LPFGs have bandwidth typically larger than ~200 GHz. Although, it is possible to process lower-bandwidth signals using the reported uniform LPFG-based differentiators, this would result in a very poor energetic efficiency (EE), as EE depends quadratically on the inverse of the input signal bandwidth. EE is defined as the power ratio between the differentiated (output) and original (input) signals. Thus, the EE is fully optimized when the input signal bandwidth matches the maximum processing bandwidth of a given differentiator. The processing window of ~20–200 GHz can be easily covered with a differentiator based on a 50/50 splitter-based Michelson interferometer [7,11]; this concept was demonstrated using a bulk-optics setup first [7], which is very inconvenient for fiber-optics applications. Moreover, thorough stabilization and/or feedback-loop may be required for reliable operation, particularly if the concept is implemented using a conventional fiber-optics interferometer [11].

Implementing the differentiation process in the 20 – 200 GHz bandwidth is highly desired in the above-mentioned applications [8–10] for telecommunication systems operating at bit rates between 40 and 160 GHz. For instance, previous flat-top pulse-based optical switching experiments using uniform LPFG-based differentiator were essentially limited to links operating above 160 GHz [9], according to the duration of the flat-top pulses that could be efficiently generated using the LPFG differentiation technique (pulses typically shorter than a few picoseconds). Another example is the recently-demonstrated simple and practical technique for phase reconstruction of an arbitrary optical signal based on photonic temporal differentiation [8]. Here, the signal-to-noise ratio (SNR) is proportional to the linear slope of the differentiation transfer function. Thus, it is very important to have an optimized differentiation bandwidth, matching the expected bandwidth of the signals to be characterized, in order to maximize the measurement SNR. Finally, a differentiator optimized for operation in the 20–200 GHz bandwidth range should also prove very useful for processing broadband RF signals, namely for microwave photonics applications, e.g. for ultra-wideband (UWB) pulse generation and processing [12].

In this paper, we propose a new structure for all-fiber photonic differentiator that is based on a common-path fiber Mach–Zehnder (MZ) interferometer operated at the destructive-interference point. The transfer function of such fiber MZ is similar to that of the Michelson interferometer demonstrated earlier for optical differentiation [7]. The two branches of the MZ interferometer are formed by the core and a cladding mode of a single-mode optical fiber. The coupling is realized using two short LPFGs. In this configuration, both interfering signals propagate along the same optical fiber and thus they are both subjected to identical environmental fluctuations, which results in considerably more robust and simple operation compared to the previously reported fiber Michelson interferometer [11]. We show that the new scheme proposed here is particularly well suited for covering the tens-of-gigahertz processing bandwidths that were difficult to achieve with previous all-fiber implementations. Previously, we proved that the reported device is suitable for various pulse shaping functionalities, like flat-top [13] or parabolic-like [14] pulse synthesis. However, for these functionalities, positive interference in the MZ was used, as opposed to the destructive interference used here for optical differentiation.

2. Principle of operation

As the here-proposed device is in fact an all-fiber implementation of a principle proposed earlier [7], it may be instructive to review first its principle of operation in the spectral domain, as explained in [7].

A symmetric (splitting/coupling ratio of 50%), imbalanced (the two interfering paths are of different lengths) interferometer has the following spectral transfer function:

$$H_t(\omega-\omega_0)\approx 1+\exp(i\omega\tau)=1+\exp[i(\omega-\omega_0)\tau]\exp(i\omega_0\tau), \quad (2)$$

where τ is the relative time delay between the two interferometer arms. Setting the interferometer to operate at a minimum transmission ($H_t(\omega-\omega_0)=0$) at the carrier frequency ($\omega=\omega_0$), it follows from Eq. (2) that

$$\tau=\pi(2m+1)/\omega_0, \quad (3)$$

where m is an arbitrary integer. Introducing this value of τ into Eq. (2) we obtain:

$$H_t(\omega-\omega_0)\approx 1-\exp[i\pi(2m+1)(\omega-\omega_0)/\omega_0]. \quad (4)$$

The function in Eq. (4) can be approximated over a sufficiently narrow bandwidth centered at ω_0 by the first terms of the Taylor series development:

$$\cos(\pi(2m+1)(\omega-\omega_0)/\omega_0)\cong 1 \text{ and } \sin(\pi(2m+1)(\omega-\omega_0)/\omega_0)\cong\pi(2m+1)(\omega-\omega_0)/\omega_0, \quad (5)$$

resulting in:

$$H_t(\omega-\omega_0)\approx -i(\omega-\omega_0)\pi(2m+1)/\omega_0, \quad (6)$$

which is the transmission function required for the temporal differentiator, Eq. (1), multiplied by a constant (device–design-related) factor of $\pi(2m+1)/\omega_0$. As follows from the above discussion, the expression in Eq. (6) strictly holds over a narrow bandwidth of frequencies (around ω_0 that satisfy the condition $(2m+1)\Delta\omega/\omega_0=\tau\Delta\omega/\pi\ll 1$, where $\Delta\omega=|\omega-\omega_0|$.

The here-proposed implementation of the symmetric imbalanced interferometer is based on an all-fiber device containing a cascade of two LPFGs that form an imbalanced symmetric MZ interferometer, Fig. 1.

The light is split by the first LPFG, then propagates in the core and cladding modes with different speeds and is superimposed coherently using the second LPFG.

The key in obtaining optical differentiation is a precise symmetry of the MZ interferometer in terms of the splitting ratios in order to obtain full destructive interference. The first LPFG couples 50% of light into a cladding mode. Subsequently, 50% of energy propagates in the cladding mode while the other 50% propagates in the core mode. The light propagating in the core mode accumulates (with respect to the cladding–propagating portion of the signal) a delay τ due to the difference in the group velocities between the core and cladding modes. As both modes propagate within the same fiber and as the interferometer length is typically of the order of a few to tens of centimeters, any environmental change influences both modes in nearly the same manner, which results in a very robust device operation. Moreover, the performance of LPFGs is almost independent on the input polarization. Thus, the filter is very weakly polarization dependent.

The considered differentiator can be understood in the temporal domain too. At the interferometer output, we get the difference

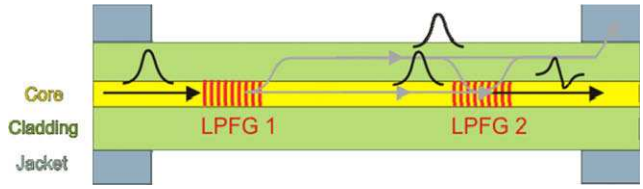

Fig. 1. Schematic of the LPFG-based MZ interferometer.

between the signal and its delayed replica by a small time τ, which is actually the mathematic definition of discrete-time differentiation (within a multiplicative factor of $1/\tau$). To obtain a precise differentiation, the time τ (relative delay induced by the MZ interferometer) has to be much shorter than the fastest temporal feature of the signal to be processed. As derived above, this condition can be mathematically expressed as follows: $\tau \ll \pi/\Delta\omega$, where we remind the reader that $\Delta\omega$ represents the spectral bandwidth of the input optical signal to be processed. However, for too small τ, the differentiator suffers from very large insertion losses, as our device gives the differentiated signal attenuated by a factor of τ (see Eq. (6)).

3. Design and fabrication of differentiator samples

The fiber cladding supports a huge amount of modes that can be used. However, only coupling to some specific cladding modes is practical. First, we have to choose modes that have large field overlap with the core mode, which translates into a higher coupling strength (requiring shorter LPFG) [15]. In a standard single-mode telecom fiber, these are typically 3rd–9th odd cladding modes (LP04–LP10) [15]. Further, for obtaining devices as short as possible (for easier stabilization and packaging), we need to maximize the difference in the group velocities between the fiber core mode and the considered cladding mode. In this way, the desired τ may be obtained with a shorter fiber length. The group velocity is given by the phase velocity (characterized by the effective refractive index of the mode, n_{eff}) and the modal dispersion [16]. For SMF-28 fiber, the higher group velocity difference is offered by the lower-order cladding modes. e.g., Using LP05, a 20-cm long structure leads to ~200-GHz bandwidth differentiator. To obtain a narrower-bandwidth differentiation with the same device length, a fiber with higher numerical aperture, leading to higher dispersion difference between the core and a well-coupling cladding mode, has to be used. In our experiments, we used SM980 (4.5/125) from FiberCore Inc., UK with N.A. = 0.14 that allowed us to achieve a differentiation bandwidth of ~100 GHz for a total length of less than 20 cm.

We prepared various samples that yield MZ with spectral periods of 1.2–6.5 nm, with corresponding differentiation bandwidth (bandwidth over which the filter transfer function has the required shape, see Eq. (1)) of 55–300 GHz. The typical LPFG length was 5–20 mm, the inter-LPFG separation 5–25 cm, the LPFG period of

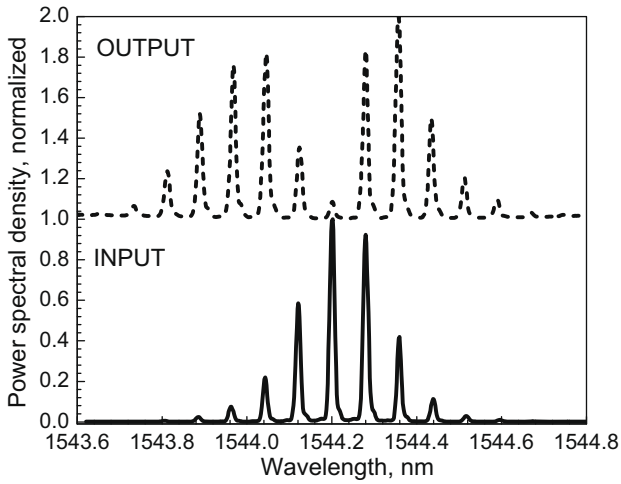

Fig. 3. Normalized spectra of the output (dashed) and the input (solid) signals. The 3-dB bandwidths are 71 and 32 GHz, while full bandwidths are 105 and 58 GHz, respectively.

490 μm (samples made in SMF-28 fiber) and 390 μm (samples made in SM980 (4.5/125)).

For the experiment, we chose a device capable of processing input signals compatible with 40-GHz telecom technology. The measured transfer function in terms of the amplitude and phase obtained with an optical vector analyzer (OVA from LUNA Inc., USA) is shown in Fig. 2. To demonstrate the device stability, the transmission spectra were acquired 128 times during 4 min and the averaged result is shown in Fig. 2. The averaged characteristics were identical to those obtained with a single-scan measurement.

Based on the spectral characteristics shown in Fig. 2, it is worth noting that due to the periodic character of the device transfer function and the fact that the transfer function of the differentiator is attained only within a fraction of one of its periods, our filter cannot easily process wavelength division multiplexed signals, which would be easier with other previously-demonstrated devices (e.g., using uniform LPFG [4] and π-FBGs [5]).

4. Results

The input signal consisted of 17-ps FWHM long Gaussian-shape pulses that were obtained by filtering a 10-GHz repetition rate

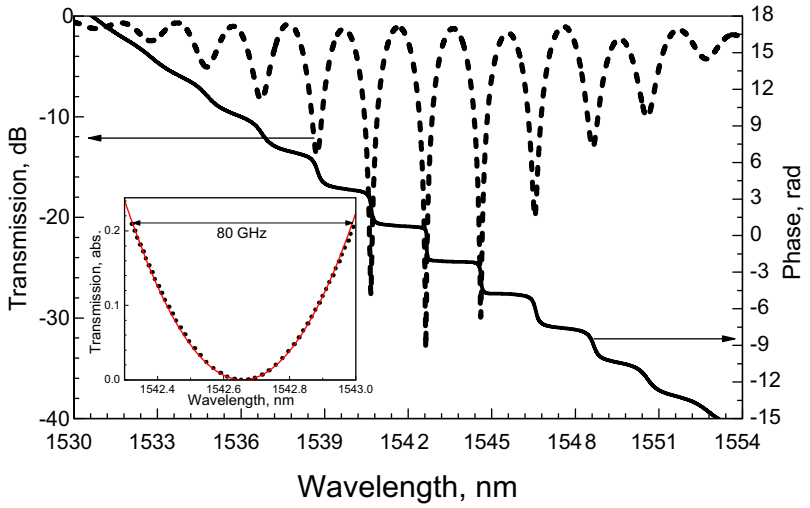

Fig. 2. Spectral power transmission and phase response of the differentiator sample made in SM980 fiber; LPFGs are 2 cm each (50 periods, Λ = 391 μm) separated by 16 cm. Inset: measured and ideal differentiator power transmission. Differentiation input bandwidth: 80 GHz.

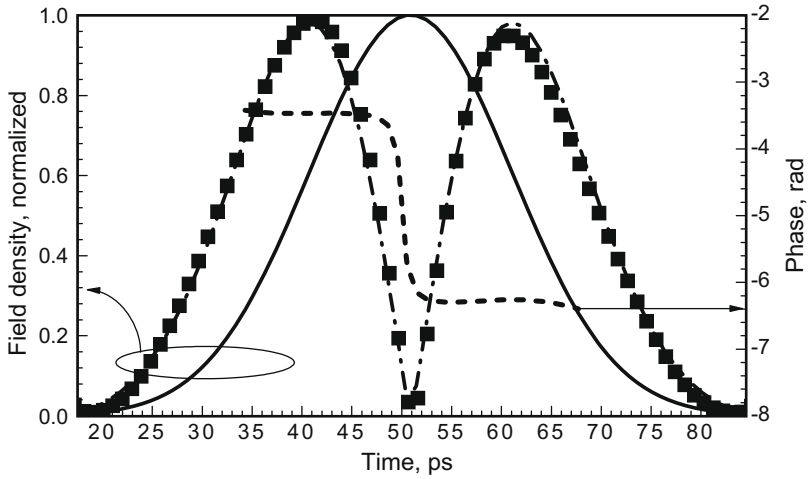

Fig. 4. Temporal characteristics in terms of the field amplitudes. The input pulse: solid line, its ideal first time derivative: dash-dot line, measured output: square ticks, measured temporal π-phase jump: dashed line.

mode-locked fiber-coupled semiconductor laser (U2t, Germany) with a tunable 0.3-nm fiber Bragg grating (FBG)-based filter (JDSU, Canada). The shape and duration of the pulses were verified via temporal autocorrelation. The generated pulses had 0.27-nm FWHM and full width (measured at 10% of its peak intensity) of 0.5 nm (corresponding to about 60 GHz). The used differentiator had ~80 GHz input bandwidth, Fig. 2. The output pulses would be very difficult to observe directly in the temporal domain, as a 100-GHz sampling scope would be needed. Thus, we performed the measurement in the spectral domain. To obtain amplitude and phase of the output signal, we used a fiber-based Fourier-transform spectral interferometry setup (in this setup, the input pulse was used as the reference pulse) [4]. For illustration purposes, the spectral characteristics of the input and output signals are shown in Fig. 3. The delay in the fiber interferometer was set to 50 ps (half of the repetition rate of the used signal), according to the requirements for Fourier-transform spectral interferometry. To obtain correct results, the phase in the measurement interferometer had to be controlled.

The result is shown in Fig. 4. The input pulse of 17 ps FWHM in optical power was processed with almost negligible processing error. The theoretically expected π-phase jump between the two lobes of the output waveform was also clearly observed. We also measured the energetic efficiency (insertion loss) by measuring the average optical power at the differentiator input and output. We measured 2.2%, which is in a very good agreement with the theoretical predictions considering the insertion loss of our in-house made differentiator to be about 0.6 dB. The expected energetic efficiency would be 2.6% when no insertion loss is considered. The maximum obtainable energetic efficiency was reported to be close to 3% – this value would be obtained for our differentiator if a signal with a full bandwidth of 80 GHz had been used.

5. Conclusions

We demonstrated a new configuration of all-fiber photonic differentiator that allows obtaining easily the tens-of-gigahertz bandwidth range, which is difficult to reach with any of the previously proposed all-fiber solutions for temporal differentiation. As an example, we fabricated and tested an 80-GHz full bandwidth differentiator. The device was successfully demonstrated by differentiating 17-ps FWHM (60-GHz full bandwidth) Gaussian optical pulses, having obtained an energetic efficiency of 2.2%. The demonstrated device should prove useful for a variety of pulse re-shaping and signal characterization applications in telecommunication systems, particularly for operation at frequencies in the 40 GHz to 160 GHz range.

Acknowledgement

This research was supported by the Grant Agency of AS CR under Contract KJB200670601 and by the Czech Science Foundation under Contract 102/07/0999.

References

[1] N.Q. Ngo, S.F. Yu, S.C. Tjin, C.H. Kam, Opt. Commun. 230 (2004) 115.
[2] M.A. Preciado, M.A. Muriel, Opt. Lett. 33 (2008) 2458.
[3] J. Xu, X. Zhang, J. Dong, D. Liu, D. Huang, Opt. Lett. 32 (2007) 3029.
[4] R. Slavík, Y. Park, M. Kulishov, R. Morandotti, J. Azaña, Opt. Express 14 (2006) 10699.
[5] N.K. Berger, B. Levit, B. Fischer, M. Kulishov, D.V. Plant, J. Azaña, Opt. Express 15 (2006) 371.
[6] J. Xu, X. Zhang, J. Dong, D. Liu, D. Huang, Opt. Lett. 32 (2007) 1872.
[7] Y. Park, J. Azaña, R. Slavík, Opt. Lett. 32 (2007) 710.
[8] F. Li, Y. Park, J. Azaña, Opt. Lett. 32 (2007) 3364.
[9] L.K. Oxenlowe, R. Slavík, M. Galili, H.C.M. Mulvad, A.T. Clausen, Y. Park, J. Azaña, P. Jeppesen, IEEE J. Sel. Top. Quantum Electron. 14 (2008) 566.
[10] Q. Wang, F. Zeng, S. Blais, J. Yao, Opt. Lett. 31 (2006) 3083.
[11] Y. Park, T.-J. Ahn, J. Azaña, Appl. Opt. 47 (2008) 417.
[12] F. Zeng, J. Yao, IEEE Photon. Technol. Lett. 18 (2006) 2062.
[13] R. Slavík, Y. Park, J. Azaña, IEEE Photon. Technol. Lett. 20 (2008) 806.
[14] R. Slavík, Y. Park, T.-J. Ahn, J. Azaña, Synthesis of picosecond parabolic pulses formed by a long period fiber grating structure and its application for flat-top suercontinuum generation, Optical Fiber Communications (OFC'08), San Diego, CA, USA, Paper OTuB4, February 2008.
[15] T. Erdogan, J. Opt. Soc. Am. A 14 (1997) 1760.
[16] B.H. Lee, J. Nishii, Appl. Opt. 38 (1999) 3450.